Diagnostic Potential of Laser-Induced Autofluorescence Emission in Brain Tissue

Laser-induced autofluorescence measurement of the brain was performed to assess its spectroscopic properties and to distinguish brain tumors from the normal tissues. The excitation-induced emission spectra were plotted on a 2-dimensional map, the excitation-emission matrix, to determine the excitation wavelengths most sensitive for the spectroscopic identification of brain tumors. The excitation-emission matrices of various types of human brain tumors and normal brain samples lead to the selection of three fluorescence peaks at 470, 520, and 630 nm, corresponding excitation light at 360, 440, and 490 nm, respectively for comparing the autofluorescence signatures of brain tissue. The fluorophores most likely related to each of these peaks are NAD(P)H, various flavins, and porphyrins, respectively. In vivo studies of rat gliomas showed that "NAD(P)H", "flavin", and "porphyrin" fluorescence were lower in gliomas than in normal brain. This finding suggests that there are certain relationship between brain tissue autofluorescence intensity and metabolic activity. In vitro human normal brain tissue fluorescence signals were lower in gray matter than in white matter and "NAD(P)H" fluorescence were lower in all measured human brain tumors than in normal brain. "Flavin" and "porphyrin" fluorescence in the neoplastic tissues was lower or higher than normal tissue depending on their nature. In conclusion, the fluorescence spectroscopic diagnostic system might be able to distinguish brain tumors from the normal brain tissue. The results of this study need to be verified and the investigation extended to human brain tumors in the operating room. ***(JKMS 1997;12:135~42)***

Key Words : *Autofluorescence, Brain tumor, Fluorophores*

Yong Gu Chung, M.D.*, Ph.D.,
Jon A. Schwartz, M.E.E., Craig M. Gardner, M.S.,
Raymond E. Sawaya, M.D.,
Steven L. Jacques, Ph.D.

Department of Neurological Surgery and Laser Biology Research Laboratory
The University of Texas M.D. Anderson Cancer Center, Houston, Texas
College of Medicine, Korea University, Seoul, Korea(*)

Received : June 24, 1996
Accepted : December 16, 1996

Address for correspondence
Yong-Gu Chung, Department of Neurosurgery, Korea University Anam Hospital, 5-Ka Anam-Dong, Sungbuk-Gu, Seoul 136-701, Korea
Tel : (02) 920-5729

INTRODUCTION

Resectability of gliomas has been shown to improve prognosis (1, 2). However, most gliomas do not have a distinct boundary, making complete resection difficult or impossible. Standard micro-neurosurgical techniques (3) and intraoperative ultrasonography (4) have been recommended for gross total resection.

Lasers have traditionally been used in medicine as therapeutic devices, and recently there has been interests using them diagnostic tools. Laser-induced fluorescence (LIF) of tissue has been studied by a number of investigators to differentiate normal arteries from areas covered by atheomatous plaque (5~9) and to distinguish tumors from the normal surrounding tissue (10~12). Tissue fluorescence arises from the superposition of the fluorescence of a number of molecules present in the tissue. The observed fluorescence spectrum depends on the characteristics of the excitation light and emitted light. It is well known that fluorescence of materials such as human tissue can provide information by the presence of very small amounts of biological chromophores (13). Preliminary reports have suggested that differences of biological chromophores in normal and neoplastic human colon can be measured using fluorescence spectroscopy, and the basis of a diagnostic test for colonic neoplasia (6, 14~16) was developed from it. It remains to be demonstrated whether the changes in tissue fluorescence spectra accompanying tumor development are sufficient to constitute a unique spectral "signature" useful for diagnostic purposes. The purpose of this study was to survey the spectroscopic properties of normal brain tissue and brain tumor to determine : 1) whether the spectroscopic properties of these tissues are sufficiently different to assist diagnosis, 2) if so, at which excitation wavelength(s) is this differentiation best achieved, and 3) the feasibility of using LIF to distinguish brain tumors from normal brain tissue in a rat model.

MATERIALS AND METHODS

Instrumentation

The autofluorescence measurement system is shown schematically in Fig. 1. The output of a pulsed nitrogen laser (VSL 337ND-T, Laser Science, Inc., Cambridge, MA) (337 nm, 3-ns pulses, 7Hz, 250 μJ/pulse) was used to pump a dye laser module (#337220, Laser Science, Inc). The output of the dye laser was tuned in 10-nm increments over the range 360~560 nm and was coupled by means of a 1-inch focal-length quartz lens into a single 300-μm-core-diameter optical fiber, which delivered excitation light to the target tissue. Pulse energies delivered to the tissue ranged from 2 to 20 μJ depending on the dye and wavelength. Fluorescence from the tissue was collected by collection fibers which were circularly arranged around the excitation fiber (see Fig. 1, inset). The distal end of the optical fiber bundle was maintained at a fixed distance of 3.6 mm from the target tissue by means of a circular spacer situated around the fiber bundle. The spacer permitted the overlap to the excitation and collection fibers' field-of-view. The collection fibers carried the fluorescence emission to the detection system where the fibers formed a rectangle of 0.1×2.5 mm which was placed against the entrance slit of a 0.32-m spectrograph (HR-320, Instruments S.A., Inc., Princeton, NJ) which consisted of a 1,024--diode array with a microchannel plate intensifying the signal from the central 700 diodes. Reflected laser light was blocked from the OMA by a long-pass filter at the entrance of the spectrograph. As the excitation wavelength was changed, the filter was changed to yield an appropriate cutoff wavelength. The intensifier was used in an ungated mode in a darkened room. Day-to-day variations in laser energy and fiber coupling efficiencies were taken into account by measuring the laser emission (J) from the central excitation fiber with a pyrometer (J9LP, Molectron Detector Inc., Portland, OR). Day-to-day variations in the sensitivity of OMA and the alignment of the fiber bundle with the entrance slit were taken into account by measuring the fluorescence from a cuvette of laser dye (fluorescein and rhodamine 6G, Sigma Chemical Co., St. Louis, MO) as a calibration standard. The OMA recorded a complete emission spectrum for each laser pulse at a particular excitation wavelength. For each measurement, 50 emission spectra were collected and averaged. Measurements were recorded over a range of excitation wavelengths from 360~630 nm in increments of 10 nm. Noise from ambient light was removed by making a measurement of the tissue without the excitation light.

This background measurement was automatically subtracted from each fluorescence measurement. New

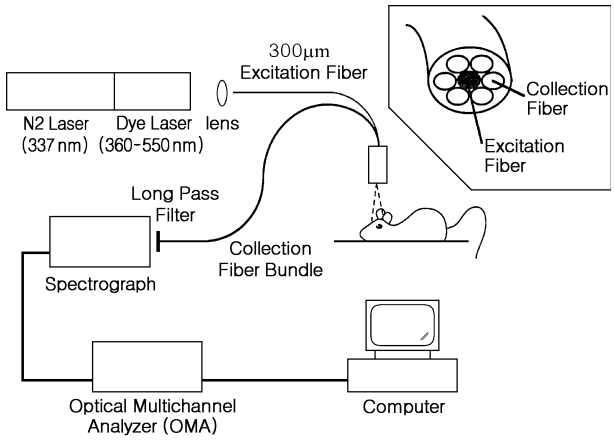

Fig. 1. Schematic diagram illustrating the laser-induced fluorescence system. A nitorgen-laser-pumped dye laser provides the tunable excitation source which is focuse into and transmitted to thd target tissue by the excitation fiber. Laser-induced autofluorescence is conducted from the target tissue to the filtered input of the spectrograph. The optical multichannel analyzer processes the autofluorescence spectrum whichis displayed and recorded by the computer. The inset shows the distal end of the fiber probe with the excitation fiber from the laser surrounde by the colletion fibers.

background measurements were made frequently in order to compensate for changes in detector sensitivity with changes in temperature and with changes th ambient light due to the insertion of different long-pass blocking filters. All spectra were system-response corrected by dividing the observed spectra by a system response curve, which was determined by measuring the spectral intensity of a calibrated 1,000-W quartz-halogen lamp (model 200 A, Optronic Laboratories Inc., Orlando, FL). The diode array was also spectrally calibrated using a low-pressure mercury lamp (model 6035, Oriel Corp., Stratford, CT). Excitation light was normally incident on the surface of the tissue specimens. Emitted fluorescence was collected from the illuminated area, approximately 3 mm in diameter at the tissue surface. Fluorescent intensities are reported here in arbitrary units relative to the intensity of the calibration standard.

Excitation/emission matrix

An exciation/emission matrix (EEM) is matrix of fluorescence emission intensities whose columns indicate emission wavelengths and rows indicate excitation wavelength. Such a matrix can be constructed from a series of emission spectra collected for a range of excitation wavelengths. An EEM is presented here as a fluorescence contour map where the y-axis indicates excitation wavelengths, the x-axis indicates emission wavelengths and contour lines connect points of equal fluorescence

emission intensity.

In vivo rat brain tissues

The C9L rat gliosarcoma cell line (American Type Culture Collection, Rockville, MD), was grown to confluence in a monolayer culture over a 5-day period, dispersed with trypsin, and suspended in Dulbecco's modified Eagle's medium at a concentration of 2×10^6 cells/10 μ1. Male CD Fisher rats, each weighing approximately 300 g, were anesthetized with an intramuscular injection of Ace promazine ketamine (1 ml/kg body weight) and secured in a stereotactic frame.

A 5×5-mm left-sided parietal craniectomy was performed on rats using a dental drill. Tumor cells were injected subcortically into the posterior parietal region in the middle of the opening via a 25 μl Hamilton syringe mounted on the stereotactic frame. A No. 30-gauge needle was inserted to puncture the dura to the point at which the beveled end, facing posteriorly, was just beneath the dura. The injection of tumor cells was carried out during a 1 minute period. The needle was kept in place for an additional 2 minutes followed by gradual withdrawal over a span of 2 minutes. The skin was closed with sutures. Ten to 14 days after inoculation, the region was re-explored to check the production of tumors and to study the autofluorescence of the tumors and normal brain tissue. Immediately after the rats were euthanized, brain samples were taken for pathological confirmation of brain tumor production.

Three types of studies of rat normal brain and tumor were performed : 1) the difference in fluorescence emission between in vivo and in vitro tissues was evaluated. 2) rat brain autofluorescence emission before and after euthanasia was studied. The rat brain autofluorescence emission of ex vivo samples stored at different temperatures for up to 72 hours after euthanasia was also studied. 3) the fluorescence of rat brain tumors and contralateral normal cerebral cortex in vivo were measured.

In vitro Human brain tumor

Solid brain tumor and normal brain specimens of different pathologic states were obtained from tumor patients during open craniotomy. The specimens were immediately transported to the laser laboratory wrapped in cotton pledges moistened with saline and studied less than 2 hours after sampling. During our studies, the tumor samples were intermittently irrigated with saline to prevent drying of the tissues. We stored the tumor specimens in different conditions to evaluate the effect of storage methods, especially temperature, on fluorescence emission. Selected brain tumor specimens were reviewed by a neuropathologist for tissue diagnosis.

Fluorescence EEM were recorded for four normal brain specimens, six anaplastic astrocytomas, two glioblastomas, two meningiomas, three low-grade astrocytomas, five metastatic tumors, one craniopharyngioma, one olfactory neuroblastoma.

In vitro GBM cell aggregates

We evaluated the autofluorescence emission of several human and rat brain tumor cell lines : UWR1, U251, SNB19, C9L, and C6BAG. Four to 5 days after subculture, the cell lines became confluent. Cell aggregates were prepared after either scrubbing or trypsinization. Comparative autofluorescence measurements were made in the prepared cell aggregates, which were typically ovoid measuring 7×5×3 mm. Autofluorescence measurements were made by depositing the cell aggregates onto a glass microscope slide and placing the fiber optic probe directly above the samples at the 3.6 mm distance. The cell aggregates were not measured in cuvettes in order to obviate the spurious fluorescence produced by the the cuvette surface. The specular reflection of excitation light directly from the surface of the cell aggregates was sufficiently diffuse so as not to induce fluorescence in the long-pass blocking filters.

RESULTS

Rat

A characterization of the ultraviolet and visible fluorescence properties of normal in vivo rat brain is presented in Fig. 2 as contour map representaion of the average fluorescence EEM of 10 normal rat cerebral cortexe. Fluorescence intensities was given in arbitrary units. In the average fluorescence EEm, normal rat cerebral cortex exhibits three fluorescence peaks at 470, 520, and 630 nm, corresponding to excitation at 360, 440, and 490 nm, respectively. Valleys can be observed near 420, 540, and 580 nm, corresponding to the principal visible wavelength absorption bands for hemoglobin.

There was a change in the fluorescence emission of rat cerebral cortex in ex vivo smaples after euthanasia. The fluorescence intensity of in vivo gray matter was lower than that of in vitro tissues.

In vitro, the fluorescence intensity was higher in rat white matter than in gray matter. Definite "porphyrin" peaks indication excitation in the wavelength range of 360 nm 420 nm were found in the white matter. These

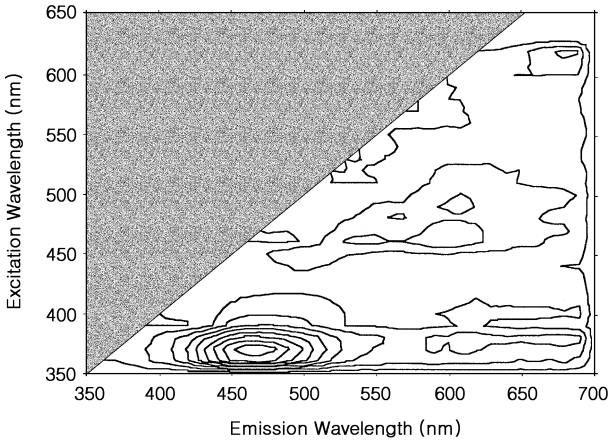

Fig. 2. Average excitation-emission matris (EEM) of 10 normal rat brains (cerebral cortex). Excitation wavelength is plotted on the ordinate, emission wavelength on the abscissa. Contour lines connect points of equal fluorescence intensity. fluorescence intensities are given in arbitrary units. Three intense fluorescence peaks ard found at excitation/emission wavelengths of 360/370 nm,440/520 nm and 490/630 nm in the EEM.

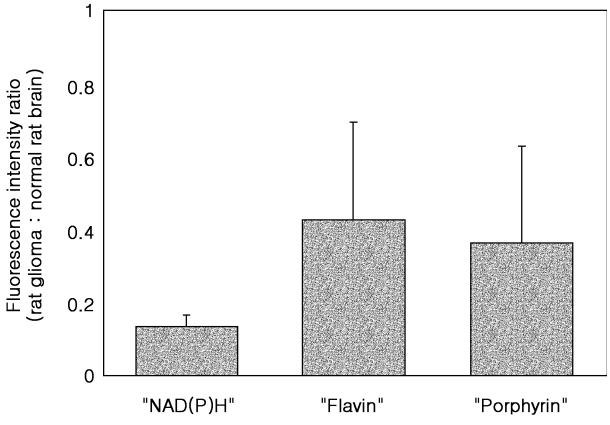

Fig. 3. Fluorescence emission in in vivo rat glioma. "NAD(P)H", "flavin" and "porphyrin" fluorescence was much lower in rat gliomas than that of normal brain. the mean ratios in fluorescence emission between the in vivo C9L glioma models and normal cerebral cortex was 0.14 for "NAD(P)H", 0.43 for "flavin", and 0.37 for "porphyrin".

"porphyrin" peaks were not observed in gray matter samples.

There were differences between the EEMs of normal in vivo rat brain with and without a blood film on the surface. In the case of normal rat brain covered with blood, the fluorescence intensities at 470, 520 and 630 nm were about one third, respectively, of those for normal brain without blood on the surface.

Fig. 3 shows the ratios in fluorescence emission between the in vivo C9L glioma models and normal cerebral cortex for 4 rats. The mean ratio for "NAD(P)H" was 0.14, the mean ratio for "flavin" was 0.43, and the mean ratio for "porphyrin" was 0.37.

As shown in Table 1, the mean ratio of "NAD(P)H" to "flavin" for the rat glioma is 4.5.

Human

Fluorescence emission results varied with the storage methods used for human tumor samples. For example, the fluorescence intensity of an astrocytoma sample stored at 4℃ was 1.8-fold higher at the 470 nm peak than that of astrocytoma stored at -72℃, but 520-nm-peak and 630 nm-peaks were nearly the same in intensity. There were some changes in the 520-nm-peak area (two additional peaks were found) for a tumor sample stored at -72℃.

Fig. 4 shows the location of peaks in the EEM for normal brain and tumors. Three groups of peaks were found. The first group was located at excitation wavelengths from 360 to 380 nm with emission from 450 to 500 nm. The second group was located at excitation wavelengths from 440 to 450 nm with emission from 500 to 550 nm. The third peak was located at excitation wavelengths from 490 to 500 nm with emission from 590 to 630 nm. Three optimal excitation/emission wavelength pairs were chosen to represent each group of peaks in a comparison of normal brain and tumor tissue : 360/470 nm, 440/520 nm, and 490/630 nm. The most likely fluorophores potentially representing these three peaks are NAD(P)H, flavin, and porphyrin respectively.

Fig. 5 shows differences in fluorescence emission between white (n=4) and gray (n=3) matter for in vitro human brain tissue. "NAD(P)H", "flavin", and "porphyrin" fluorescence signals were higher in white matter than in gray matter. The ratios of white to gray matter

Table 1. Ratio of "NAD(P)H" to "flavin" for *in vivo* and *in vitro* studies.

Tissue type	Mean	Standard dev.	Number (n)
Normal human brain *(in vitro)*	4.3	2.9	4
GBM pellet (1)	5.0	1.2	3
GBM pellet (2)	9.9	5.2	4
Metastasis	5.8	1.5	4
GBM	6.0	0.5	2
LG astrocytoma	4.1	1.6	3
HG astrocytoma	10.3	3.4	6
Rat glioma *(in vivo)*	4.5	2.1	7
Normal rat brain *(in vivo)*	5.0	3.9	9

GBM (1) : GBM cell pellet prepared with scrubbing
GBM (2) : GBM cell pellet prepared with trypsin-EDTA

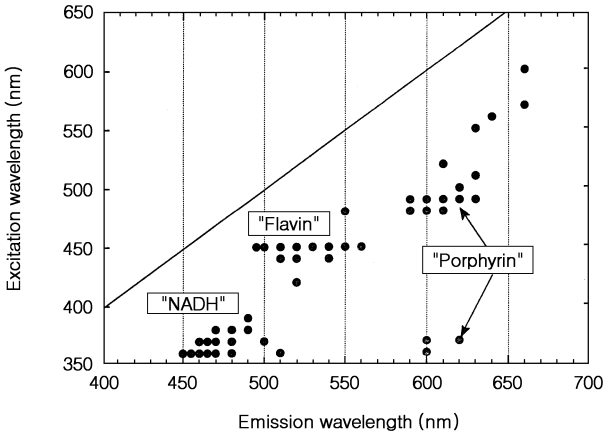

Fig. 4. Location of peaks on the EEM of normal human brain and brain tumors. Three groups of peaks were found. The first group was located at excitation wavelengths from 360 nm to 380 nm with emission from 450 nm to 500 nm. The second group was located at excitation wavelengths from 440 to 450 nm with emission from 500 nm to 550 nm. The third peak was located at excitation wavelengths from 490 nm to 500 nm with emission from 590 to 630 nm. There are several fluorophores that potentially represent each peak. However, the fluorophores most likely related to each peak are NAD(P)H, flavin, and porphyrin, respectively.

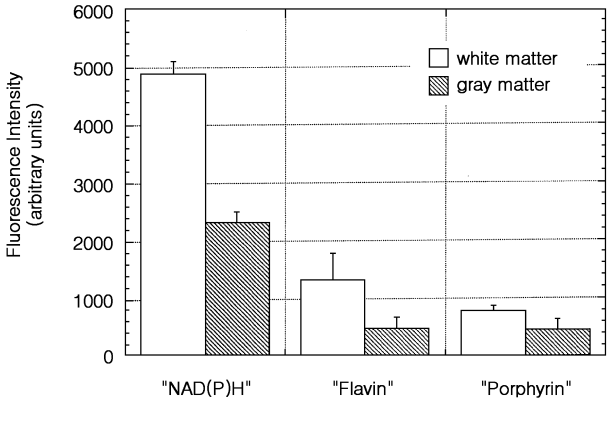

Fig. 5. Fluorescence emission in normal in vitro human brain tissue. "NAD(P)H", "flavin" and "porphyrin" fluorescence signals are higher in white matter than in gray matter in ratios of 2.1:1 for "NAD(P)H", 2.68:1 for "flavin", and 1.69:1 for "porphyrin". Fluorescence intensities of "NAD(P)H", "flavin", and "porphyrin" exist in ratios of 6.2:1.7:1.0 respectively for white matter, and 5.0:1.1:1.0 respectively for gray matter.

fluorescence intensities were 2.1:1 for "NAD(P)H", 2.68:1 for "flavin", and 1.69:1 for "porphyrin", and "porphyrin" exist in ratios of 6.2:1.7:1.0 respectively for white matter, and 5.0:1.1:1.0 respectively for gray matter.

The fluorescence spectra of normal brain and different kinds of brain tumors are shown in Fig. 6. The "NAD(P)H" fluorescence intensity of normal in vitro brain tissue was larger than that measured in metastatic tumors, low-and high-grade astrocytomas, and medulloblastoma. "Flavin" fluorescence was less than that of normal brain tissue in metastatic tumors and low-grade astrocytoma, but higher than that of normal brain tissue in medulloblastoma. "Porphyrin" fluorescence was much less than that of normal brain in metastatic tumors and low-grade astrocytoma but nearly equal to or slightly higher than that of normal brain in medulloblastomas and high-grade astrocytomas.

Table 1 gives comparisons of the fluorescence peaks for rat, human, and GBM aggregate samples where the ratio of the "NAD(P)H" peak (excitation/emission=360/470 nm) to the "flavin" peak (440/520 nm) is shown. The ratios of "NAD(P)H" to "flavin" peaks ranged from 1.6 to 9.2 with a mean of 4.3 in normal human in vitro brain. The mean ratios of NAD(P)H" to "flavin" of the low grade astrocytoma and the metastasis are 4.1 and 5.8 respectively. But the corresponding ratios for high grade astrocytomas and the GBMs are 10.3 and 6.0,

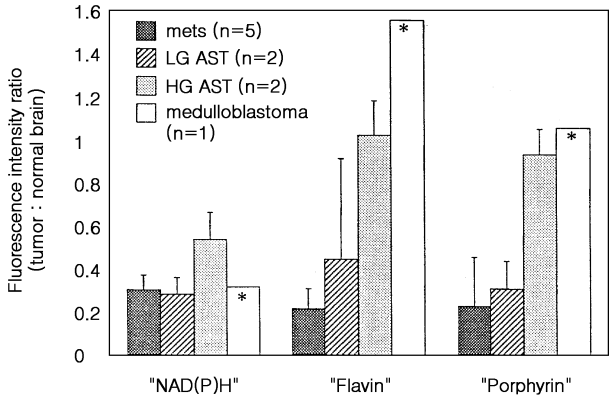

Fig. 6. The fluorescence spectra of normal human brain and different kinds of brain tumors. The "NAD(P)H" fluorescence intensity of normal in vitro brain tissue was greater than that of brain tumors. "Flavin" fluorescence of metastatic tumors and low-grade astrocytomas was less than that of normal brain except in medulloblastoma, where it was higher than that of normal brain. "Porphyrin" fluorescence of metastatic tumors and low-grade astrocytomas was much less than that of normal brain, except in the cases of medulloblastoma and high-grade astrocytoma; in these tumors, "porphyrin" fluorescence was nearly equal to or slightly greater than that of normal brain.

respectively.

GBM cell aggregates

The three fluorescence peaks were also measured in GBM cell aggregates. As shown in Table 1, the mean ratio of "NAD(P)H" to "flavin" for the GBM pellet

prepared with scrubbing is 5.0 but, the ratio in the GBM pellet prepared with trypsin-EDTA is 9.9.

DISCUSSION

Numerous investigators have suggested the tissue autofluorescence for a diagnostic tool (5~14, 17). However, many problems must be worked out before LIF can be used clinically.

This study has shown that the excitation/emission wavelengths optimal for spectroscopic differentiation between normal brain and brain tumor are 360/470 nm, 440/520 nm, and 490/630 nm. By measuring the fluorescence intensity at these three peaks, one can possibly identify a brain tumor with a high degree of accuracy. Potential tissue fluorophores were identified by comparing our measured excitation/emission peaks with those cited in the literature (18, 19) (Table 2). Note that the band positions of potential fluorophores may not exactly match our tissue band positions. Several effects may be responsible for these differences. It is known that the fluorescence spectra of turbid tissues depend on both the emission of tissue fluorophores and the wavelength-dependent collection of this emission which is attenuated by tissue absorption and scattering (13, 15, 20).

Attenuation affects both the observed locations of the excitation/emission maxima and the observed peak shapes of individual tissue fluorophores in the multicomponent tissue EEM. Also, the observed shapes and positions of chromophore maxima can be altered in multicomponent tissue EEM when the excitation and emission peaks of individual chromophores closely overlap. In addition, since the fluorescence of molecules depends of their physical environment, including pH, solvation, and oxidation state, the fluorescence data obtained from resected or dead tissue may not accurately represent the in vivo or living situation. Furthermore, the spectroscopic properties of many fluorophores are dependent on local environmental factors such as pH and temperature. Potential fluorophores for the tissue peaks at 360/470 nm, 440/520 nm, and 490/630 nm include "NAD(P)H", "flavoproteins", and "porphyrins", respectively. The NAD(P)H molecules play a widespread role as coenzymes to many dehydrogenase enzymes both in the cytosol and within the mitochondria. They are therefore key components of many metabolic pathways affecting carbohydrate, lipid, and amino acid metabolism. Generally, NAD-linked dehydrogenases catalyze oxidation- reduction reactions in oxidative pathways, e.g., the citric acid cycle, whereas NADP-linked dehydrogenases are found in pathways concerned with reductive synthesis, e.g., the pentose phosphate pathway.

Table 2. Maximum excitation and emission wavelengths for common biological fluorophores.

Fluorophore*	Excitation wavelength (nm)	Emission peak wavelength (nm)
NAD(P)H	340	460
FAD	460	520
PP IX	390	630

*Abbreviations: NADH=nicotinamide adenine dinucleotide; FAD=flavin adenine dinucleotide; PPIX=protoporphyrin IX. (Adapted from Schomacker, et al, [1992]).

Riboflavin consists of a heterocyclic isoalloxazine ring attached to the sugar alcohol ribitol. It is a colored, fluorescent pigment that is relatively stable in heat but decomposes in the presence of visible light. Active riboflavins are flavin mononucleotide (FMN) and flavin adenine dinucleotide (FAD). Enzymes known as flavoproteins utilize the flavins and serve as several important oxidoreductases in mammalian metabolism. In their roles as coenzymes, flavins undergo reversible reduction of the isoalloxazine ring to yield the reduced forms FMNH2 and FADH2. Using fluorescence signals of "NAD(P)H" and flavoprotein, the redox states of cytosolic and mitochondrial NAD Systems can be identified. As shown in Fig. 7 which is adapted from Halangk and Kunz (21) when lactate is added to normosic epididymal spermatozoa to depress metabolism, a large increase of the "NAD(P)H" fluorescence and a decrease of the flavoprotein fluorescence are observed. If caffeine is then added to stimulate metabolism, a measurable decrease of NAD(P)H and an increase of flavoprotein fluorescence

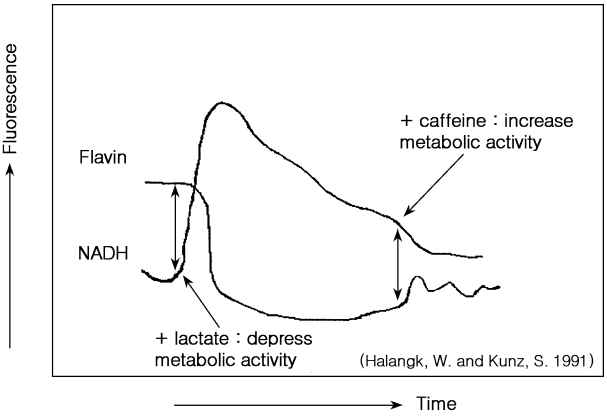

Fig. 7. Effect of caffeine on NAD(P)H and flavoprotein fluorescence in intact spermatozoa (W Halangk and W Kunz, 1991). Administration of lactate to depress metabolism increases NAD(P)H fluorescence and decreases flavoprotein fluorescence. Administration of caffeine to stimulate metabolism decreases NAD(P)H fluorescence and increases flavoprotein fluorescence.

signals occur. NAD(P)H and flavin fluorescence signals may be closely related to cellular metabolic activity. The "NAD(P)H" and "flavin" fluorescence signals were less in gray matter than in white matter for in vitro normal human brain samples. However, from previous work (21), and because the ratio of "NAD(P)H" fluorescence to "flavin" fluorescence was higher in gray matter than in white matter we may infer that metabolic activity of the gray matter is lower than that of white matter for in vitro human normal brain. Similarly, the in vitro metabolic activity of the metastatic tumors may be lower than those of low-and high-grade astrocytomas and medulloblastomas (Fig. 6).

"NAD(P)H" and "flavin" fluorescence signals were much lower in rat glioma models than were those of normal rat brain (Fig. 3). In vivo, the mean value of the ratios of "NAD(P)H" to "flavin" was also lower in gliomas than in normal brain (Table. 1). However, there were a great deal of variation in the ratios for normal brain. Thus it may be hard to differentiate gliomas from normal brain by measuring the ratios of "NAD(P)H" to "flavin" fluorescence in vivo.

There were no remarkable differences in the ratios of "NAD(P)H" to "flavin" between in vitro human normal brain and tumors, except for anaplastic astrocytomas and GBM cell aggregates prepared with trypsin. This observation seems general, having been observed in other tissues as well. e.g., Richards-Kortum et al., found that the peaks assigned to NAD(P)H and pyridoxal-5-phosphate are twice as intense in normal colonic tissue as in adenomatous tissue (15).

Schomacker et al., found that the predominant changes in the fluorescence spectra for hyperplastic adenomatous polyps compared with normal tissue are a decrease in collagen fluorescence and a slight increase in hemoglobin reabsorption (16). Yuanlong et al. (12) and Richards-Kortum et al. (15) have found that peaks assigned to porphyrin were higher in colonic adenomas and cancer than in normal tissues. However, Schomacker et al., did not find a relationship between the presence of porphyrins and polyp histology in colonic tissue. It is interesting to note that in our study, the "porphyrin" fluorescence signal was much stronger for human in vitro normal brain and rat in vivo normal brain than for brain tumors. At this point, it is hard to explain these contradictory results.

It is well known that the absorption spectrum of oxyhemoglobin exhibits peaks near 280, 350, 420, 540, and 580 nm. Thus, nearly all of the attenuation peaks noted in the total reflectance spectra of normal brain and brain tumor tissue could be ascribed to oxyhemoglobin. It is therefore impossible to get information about intrinsic (endogenous) fluorophore concentrations in the tissue without correction for blood factors. It should be noted that differences in "NAD(P)H", "flavin", and "porphyrin" fluorescence between normal brain and brain tumor tissue are not solely based on features of tissue architecture. Superficial blood, for example will selectively absorb incident excitation light and reabsorb emitted fluorescence, reducing the measured signal.

Autofluorescence is potentially ideal for tissue diagnosis because it does not require the administration of any exogenous fluorescent dyes to the patient. It may be possible, however, to achieve higher diagnostic accuracies by using fluorescent dyes specific to tumors. Dyes emitting in the spectral region>700 nm, where interference from autofluorescence is negligible, would be optimal, and are being studied in conjunction with the development of new photosensitizers for photodynamic therapy. For example, recent LIF investigations of the localization of aluminum sulfonated phthalocyanine within colonic tumors (22) and detection of 1-mm-diameter colonic tumors using a hematoporphyrin derivative (23) suggest more sensitive detection schemes.

REFERENCES

1. Ammirati M, Vick N, Liao Y. *Effect of the extent of surgical resection on survival and quality of life in patients with supratentorial glioblastoma and anaplastic astrocytomas. Neurosurgery 1987; 21 : 201-6.*
2. *MRC(Medical Research Council) Brain Tumor Working Party. Prognostic factors for high-grade malignant gliom : development of a prognostic index. J Neurooncol 1990; 9 : 47-55.*
3. Harsh GR IV, Wilson CB. *Neuroepithelial tumors of the adult brain. In : O JR, ed. Neurological Surgery, 3rd ed . Philadelphia : WB Saunders, 1990; 3040-136.*
4. Chandler WF, Knake JE, McGillicuddy JE. *Intraoperative use of real-time ultrasonography in neurosurgery. J Neurosurg 1982 ; 57 : 157-63.*
5. Anderson PS, Gustafson A, Stenram U. *Diagnosis of arterial atherosclerosis using laser-induced fluorescence. Lasers Med Sci 1987a; 2 : 261-6.*
6. Crilly RJ, gunther S, Motamei M. *Fluorescence spectra of normal and atherosclerotic human aorta : optimum discriminant analysis. Proc SPIE 1989; 1067 : 110-9.*
7. Deckelbaum LI, Lam JK, Cabin HS. *Discrimination of normal and atherosclerotic aorta by laser-induced fluorescence. Lasers Surg Med 1987; 7 : 330-5.*
8. Gaffney EJ, Clarke RH, Lucas AR. *Correlation of fluorescence emission with the plaque content and intimal thickness of atherosclerotic coronary arteries. Lasers Surg Med 1989; 9 : 215-28.*
9. Richards-Kortum RR, Rava RP, Fitzmaurice M. *A one layer model of laser induced fluorescence for diagnosis of disease in human tissue : application to atherosclerosis. IEEE Trans*

Biomed Eng 1989b ; 36 : 1222-32.

10. Alfano RR, Tang GC, Pradhan A. *Fluorescence spectra from cancerous and normal human breast and lung tissue. IEEE J Quant Elect QE-23 1987 ; 23 : 1806-11.*
11. Anderson PS, Kjellin E, Montan E. *Autofluorescence of various rodent tissues and human skin tumor samples. Lasers Med Sci 1987b ; 2 : 41-9.*
12. Yuanlong Y, Yanming Y, Fuming L. *Characteristic autofluorescence for cancer diagnosis and its origin. Lasers Surg Med 1987 ; 7 : 528-32.*
13. Richards-kortum RR, Rava RP, Cothren R. *A model for extraction of diagnostic information from laser-induced fluorescence spectra of human artery wall. Spectrochim Acta 1989a ; 45A : 87-93.*
14. Cothren RM, Richards-Kortum RR, Sivak MV. *Gastrointestinal tissue diagnosis by laser induced fluorescence spectroscopy at endoscopy. Gastrointest Endosc 1990 ; 36 : 105-11.*
15. Richards-Kortum RR, Rava RP, Petras RE. *Spectroscopic diagnosis of colonic dysplasia. Photochem Photobiol 1991 ; 53 : 777-86.*
16. Schomacker KT, Frisoli JK, Compton CC. *Ultraviolet laser-induced fluorescence of a colonic tissue : basic biology and diagnostic potential. Lasers Surg Med 1992 ; 12 : 63-78.*
17. Kapadia CR, Cutruzolla FW, O'Brian KM. *Laser-induced fluorescence spectroscopy of human colonic mucosa. Gastroenterology 1990 ; 99 : 150-7.*
18. Wolfbeiss OS, Leiner MI. *Mapping of the total fluorescence of human blood serum as a new method for its characterization. Anal Chim Acta 1985 ; 167 : 203-15.*
19. Chung-Ho, Duzma SE, Mellott J. *Spectroscopic, morphologic, and cytotoxic studies on major fraction of hematoporphyrin derivative and photofirin II. Lasers Surg Med 1987 ; 7 : 171-9.*
20. Keijzer M, Richards-Kortum RR, Jacques SL. *Fluorescence spectroscopy of turbid media: autofluorescence of human aorta. Appl Optics 1989 ; 28 : 4286-92.*
21. Halangk W, Kunz S. *Use of NAD(P)H and flavoprotein fluorescence signals to characterize the redox state of pyridine nucleotide in epididymal bull spermatozoa. Biochim Biophys Acta 1991 ; 1056 : 273-8.*
22. Tralau CJ, Barr H, Sandeman DR. *Aluminum sulfonated phthalocyanine distribution in rodent tumors of the colon, brain, and pancreas. Photochem Photobiol 1987 ; 46 : 777-81.*
23. Bjorkman DJ, Samowitz WS, Brigham EJ. *Fluorescence localization of early colonic cancer in rat by hematoporphyrin derivative. Lasers Surg Med 1991 ; 11 : 263-70.*